

## Article

# Using Simple LSTM Models to Evaluate Effects of a River Restoration on Groundwater in Kushiro Wetland, Hokkaido, Japan

Takumi Yamaguchi <sup>1</sup>, Hitoshi Miyamoto <sup>1,\*</sup>  and Tetsuya Oishi <sup>2</sup>

<sup>1</sup> Department of Civil Engineering, Shibaura Institute of Technology, 3-7-5 Toyosu, Koto-ku, Tokyo 135-8548, Japan

<sup>2</sup> Civil Engineering Research Institute for Cold Region, Public Works Research Institute, 1-34 Hiragishi 1-Jo 3-Chome, Toyohira-Ku, Sapporo, Hokkaido 062-8602, Japan

\* Correspondence: miyamo@shibaura-it.ac.jp

**Abstract:** Wetland ecosystems with proper functioning provide various ecosystem services. Therefore, their conservation and restoration are of fundamental importance for sustainable development. This study used a deep learning model for groundwater level prediction to evaluate a wetland restoration project implemented in the Kushiro Wetland in Japan. The Kushiro Wetland had been degraded due to river improvement work. However, in 2010, a wetland restoration project was carried out to restore the meandering river channel, and a decade has passed since its completion. In this study, the wetland restoration project was evaluated by comparing the response of the groundwater level using a model that reproduced physical conditions with different characteristics before and after the restoration. At first, a deep learning model was created to predict groundwater levels pre- and post-restoration of a meandering river channel using observation data. Long short-term memory (LSTM) was used as the deep learning model. The most important aspect of this study was that LSTM was trained for each of the pre- and post-restoration periods when the hydrological and geological characteristics changed due to the river channel's restoration. The trained LSTM model achieved high performance with a prediction error of the groundwater levels within 0.162 m at all observation points. Next, the LSTM models trained with the observation data of the post-restoration period were applied to evaluate the effectiveness of the meandering channel restoration. The results indicated that the meandering channel restoration improved hydrological processes in groundwater levels, i.e., their rainfall response and average groundwater water levels. Furthermore, the variable importance analysis of the explanatory variables in the LSTM model showed that river discharge and precipitation significantly contributed to groundwater level recovery in the Kushiro Wetland. These results indicated that the LSTM model could learn the differences in hydrological and geological characteristics' changes due to channel restoration to groundwater levels. Furthermore, LSTM is a data-driven deep learning model, and by learning hydrological and geological conditions to identify factors that may affect groundwater levels, LSTM has the potential to become a powerful analysis method that can be used for environmental management and conservation issues.



**Citation:** Yamaguchi, T.; Miyamoto, H.; Oishi, T. Using Simple LSTM Models to Evaluate Effects of a River Restoration on Groundwater in Kushiro Wetland, Hokkaido, Japan. *Water* **2023**, *15*, 1115. <https://doi.org/10.3390/w15061115>

Academic Editors: Mohamed M. Hantush, Latif Kalin and Rutineia Tassi

Received: 5 February 2023

Revised: 8 March 2023

Accepted: 11 March 2023

Published: 14 March 2023



**Copyright:** © 2023 by the authors. Licensee MDPI, Basel, Switzerland. This article is an open access article distributed under the terms and conditions of the Creative Commons Attribution (CC BY) license (<https://creativecommons.org/licenses/by/4.0/>).

## 1. Introduction

Wetland ecosystems provide important and essential services for humans [1,2]. These services are diverse, including flood protection, water storage, water purification, food chain support, juvenile feeding place creation, freshwater fish resource conservation, biodiversity conservation, carbon storage, and climate regulation [3,4]. Since the proper functioning of wetland ecosystems provides these ecosystem services, the conservation and restoration of wetland ecosystems are of great importance for sustainable development [5–7].

From the beginning of the 20th century to the present, especially since 1970, wetlands in many parts of the world have lost their original functions due to the effects of human activities such as water withdrawal, social infrastructure development, land development, eutrophication, invasive alien species, and climate change [3,5]. Therefore, many conservation and restoration studies have been conducted in wetland ecosystems around the world: for example, in the United States [8,9], the United Kingdom and Hungary [10], Poland [11,12], and Germany [13].

This study examined the wetland restoration project in the Kushiro Wetland, which is a representative nature restoration project in Japan, along with those in the Tama River and Lake Kasumigaura [14]. The Kushiro Wetland underwent a meandering channel restoration from 2006 to 2011, and evaluation studies were conducted immediately after the restoration [15,16]. However, there are still areas where trees have become overgrown and the grassland marsh has not yet recovered, even now, a decade after the restoration project's completion. Therefore, it is important to verify the effects of meandering channel restoration from a current scientific perspective.

Hydrological conditions are important for wetland conservation [10,17,18]. In particular, restoring the groundwater level is essential for restoring wetland vegetation [19–21]. In hydrology, simulations using physical process models have been the mainstream so far [22–25]. However, conventional hydrological models are complex, computationally intensive, and difficult for environmental management professionals to use. In particular, a groundwater flow model requires specialized knowledge and time to construct because the flow field conditions, such as its meteorology, hydrology, and geology, are complex. Therefore, introducing data-driven deep learning models [26,27] could complement physical process models, resulting in progress in our understanding of wetland conservation and management.

This study attempted to use a data-driven model to learn about changes in hydrologic and geologic characteristics due to channel restoration. The most important aspect of this study was that a data-driven model was trained for each of the pre- and post-restoration periods when the hydrological and geological characteristics changed as a result of the river channel's restoration. In this study, we used deep learning. Deep learning is a technique that aims to mimic the mammalian brain [28]. That is, it reproduces the brain's ability to transmit signals through a complex hierarchical structure. An important aspect of deep learning is that the layers of its complex structure are not designed by humans [29]. Deep learning provides a non-linear "black box" modeling approach for simulation and prediction [30].

In recent years, the use of the machine and deep learning in hydrology has exploded [31–34], and long short-term memory (LSTM) models have increasingly been used in the field of groundwater hydrology [33,34]. Table 1 summarizes a list of recent machine and deep learning studies, including uses of LSTM, in groundwater hydrology. LSTM and its modifications have been applied in many cases since 2018 to predict groundwater levels. Furthermore, comparison with other machine learning models also confirms that LSTM models effectively predict groundwater level time series.

This study differs from the development studies of new LSTM models listed in Table 1. In this study, a simple LSTM model, the performance of which has been demonstrated in many studies, was trained for both the pre- and post-restoration periods of meandering channels in the Kushiro Wetland. The objective of this study was to identify changes in the characteristics of groundwater level fluctuations by using these two LSTM models trained with different hydrological and geological conditions before and after the river channel's restoration.

First, we developed an LSTM model to predict groundwater levels before and after the meandering channel restoration with observation data. Then, using the developed pre- and post-restoration prediction models, we quantitatively evaluated whether the groundwater level recovered before and after the restoration of the meandering channel and verified the effectiveness of the restoration project. Furthermore, we analyzed the importance of the

explanatory variables used in the deep learning model, examining the meteorological and hydrological quantities that affect groundwater level changes in the Kushiro Wetland.

**Table 1.** List of the recent machine and deep learning research, including uses of LSTM, in the field of groundwater hydrology.

Region/Country	Models	Purpose	Best Model	Reference
Hetao Irrigation District in China	LSTM, FFNN	Model development	$R^2$ : 0.789–0.952	[35]
Pohang Gibuk in Republic of Korea	LSTM, NARX-DNNs, GRU, ARX	Model comparison	LSTM and NARX-DNNs	[36]
Virginia in United States	LSTM, RNN	Model comparison	LSTM	[37]
Otway and Murray Basins in Australia	LSTM, LR, MLP	Model comparison	LSTM	[38]
Republic of Korea	LSTM with PCA	Model development	Optimal input data, window size	[39]
Hebei Province in China	LSTM with WT	Model development	NSE: 0.819	[40]
Jiangsu Province in China	LSTM with KNN and WT	Model comparison	KNN-LSTM	[41]
Shandong Province in China	Convolutional LSTM, etc.	Model comparison	Convolutional LSTM	[42]
Varuna River basin in India	Bidirectional LSTM	Model development	Comparison of 5 model settings	[43]
Miandoab Plain in Iran	Bidirectional LSTMs	Model development	Double-Bidirectional LSTM	[44]
Central Europe/Rhine River	LSTM, CNNs, NARX	Model comparison	LSTM, CNNs for larger datasets.	[45]
Europe	LSTM	Model development	water table depth < 3 m	[46]
California in United States	LSTM, MLP, RNN, CNN	Model comparison	MLP	[47]
Texas in United States	LSTM-NN, simple NN	Model comparison	LSTM-NN	[48]
Anseongsi area in Republic of Korea	LSTM with CNN	Model development	AUC > 0.8 for all locations	[49]

Notes: ARX: auto-regressive exogenous. AUC: area under the receiver operating characteristics curve. CNN: convolutional neural network. DNN: deep neural network. FFNN: feed-forward neural network. GRU: gated recurrent unit. KNN: K-nearest neighbor. MLP: multi-layer perception. NARX: non-linear auto-regressive exogenous. NN: neural network. PCA: principal component analysis. RNN: recurrent neural network. WT: wavelet transform.

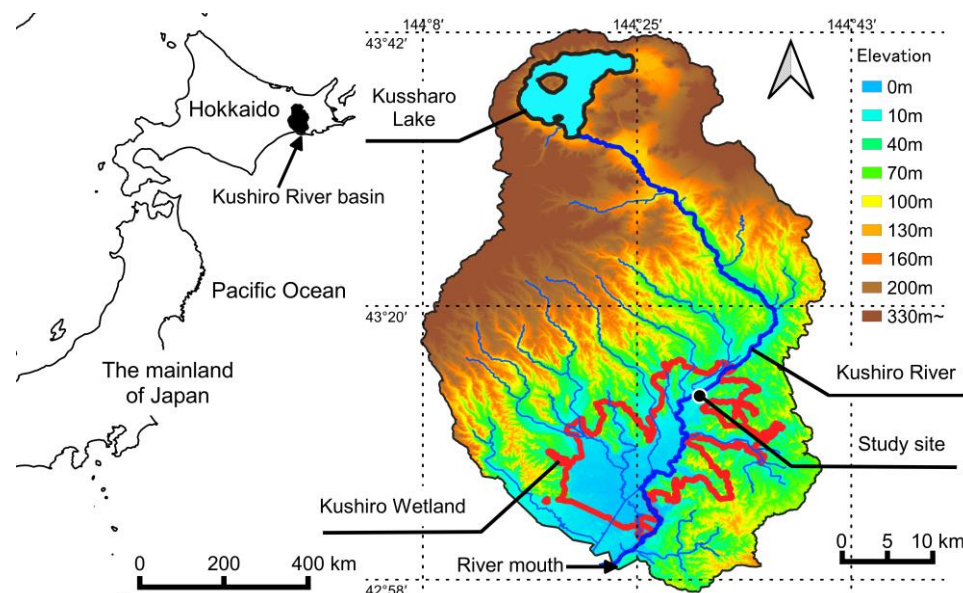
## 2. Materials and Methods

### 2.1. Target Site

As shown in Figure 1, the Kushiro Wetland is in the lower reach of the Kushiro River, which originates from Lake Kussharo. The Kushiro River basin drains an area of 2510 km<sup>2</sup> with the main channel being 154 km in length with a bed gradient of 0.001. The Kushiro Wetland is located in the southern part of the Kushiro River basin. Its area is approximately 260 km<sup>2</sup>. We conducted our study in a part of the Kushiro Wetland near the outlet of the Kushiro River on the Island of Hokkaido, Japan. Climate normals near the target site (1991–2020) [50] indicate an annual precipitation of 1054.9 mm, an average temperature of 18.4 °C in the warmest month (August) and −7.9 °C in the coldest month (January), and a maximum annual snow depth of 59 cm. A cool and humid spring and summer and dry winters with little snowfall characterize the region. The Kushiro Wetland is Japan's first registered wetland under the Ramsar Convention [51] and is Japan's largest peat grassland wetland that serves as an important habitat for wildlife. The main vegetation in the Kushiro

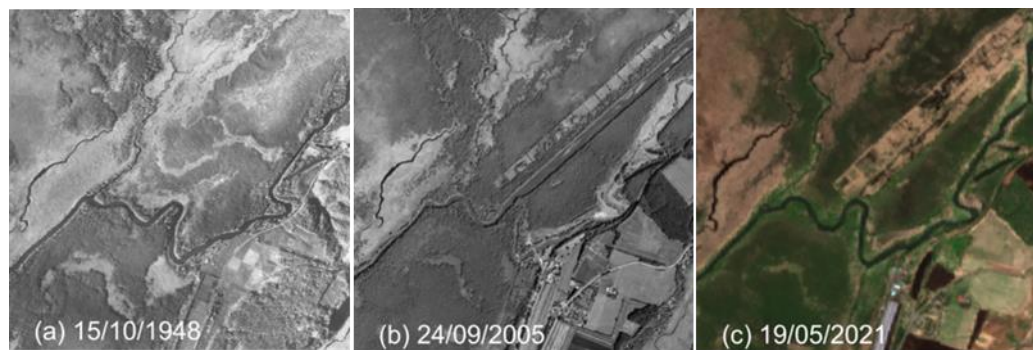
Wetland includes alder (*Alnus japonica*), reed (*Phragmites australis*), moss (*Polytrichum* spp., *Sphagnum* spp.), sedge (*Eriophorum vaginatum*), willow (*Salix* spp.), Japanese ash (*Fraxinus mandshurica* var. *japonica*), and meadowsweet (*Spiraea salicifolia*) [52].

The Kushiro Wetland has been developed for a long time; since the 1880s, there have been changes in land-use types to urban and agricultural uses. In the 1970s and 1980s in particular, meandering rivers were straightened in the northern part of the wetland to protect agricultural lands from flooding. As a result, flood flows, whose transport capacity became increased by straightening, carried sediment and nutrients from upstream agricultural lands into the wetland interior [52,53]. These sediments and nutrients changed the moisture characteristics and plant composition of the wetland, resulting in a significant transformation of the previous wetland environment. The Kushiro Wetland became drier, and shrubland species, mainly alder, flourished. Therefore, in the 2000s, the Japanese administration implemented a nature restoration project to restore the previous wetland environment through the restoration of meandering stream channels [15,16].



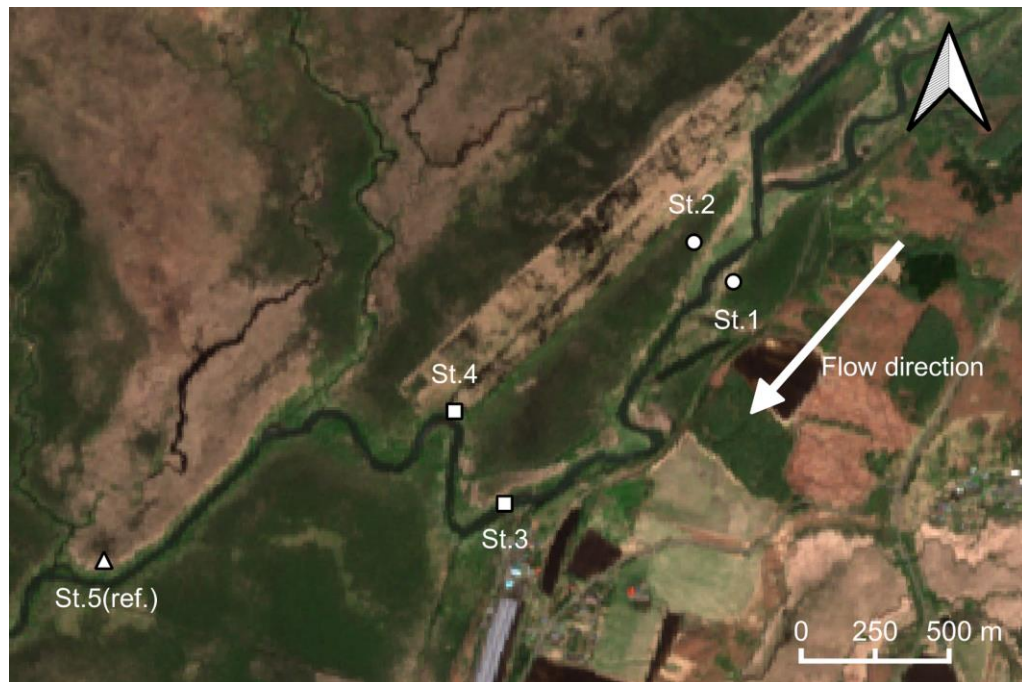
**Figure 1.** The Locations of the Kushiro River basin, Kushiro Wetland, and the study site area. Source: modified from the data in National Geodetic Data Download Service (administrative area, watershed/non-watershed boundary, natural park area, lake, and river) [54]. 1:10 m from Natural Earth by Physical Vectors Coastline.

The study site is located 30–33 km from the mouth of the Kushiro River, in the northeastern part of Kushiro Wetland, as shown in Figure 1. It is a site close to the Kayanuma railway station, where the meandering stream channel has been restored. Aerial photographs of the study site indicate contrasting situations in three different times shown in Figure 2: near pristine marshland in 1948; marshland after the straightening of the river channel in 2005; and marshland after the restoration of the meandering stream channel in 2021. In the study site, the river channel was straightened in 1984. As a result, the river and groundwater levels lowered, and the frequency of flood inundation decreased. The marshland vegetation was transformed accordingly, with reed communities being replaced by alder forests. In response to this alteration, the Japanese administration restored the study site between 2006 and 2011, replacing the straight river channel again with the meandering stream channel in 2010 as a part of the restoration project. Monitoring is currently ongoing to verify the effectiveness of the meandering channel restoration. However, as shown in the 2021 aerial photograph of Figure 2, alder forests continuously thrive in parts of the study site.



**Figure 2.** Historical changes in the study site of Kushiro Wetland from aerial images. These aerial images cover 2 km square centered at  $43^{\circ}12' N$ ,  $144^{\circ}30' E$  ((a): 15 October 1948, (b): 24 September 2005, Source: modified from the image in Geospatial Information Authority of Japan [55]), ((c): 19 May 2021, Source: modified from the image in Google Earth Engine [56]).

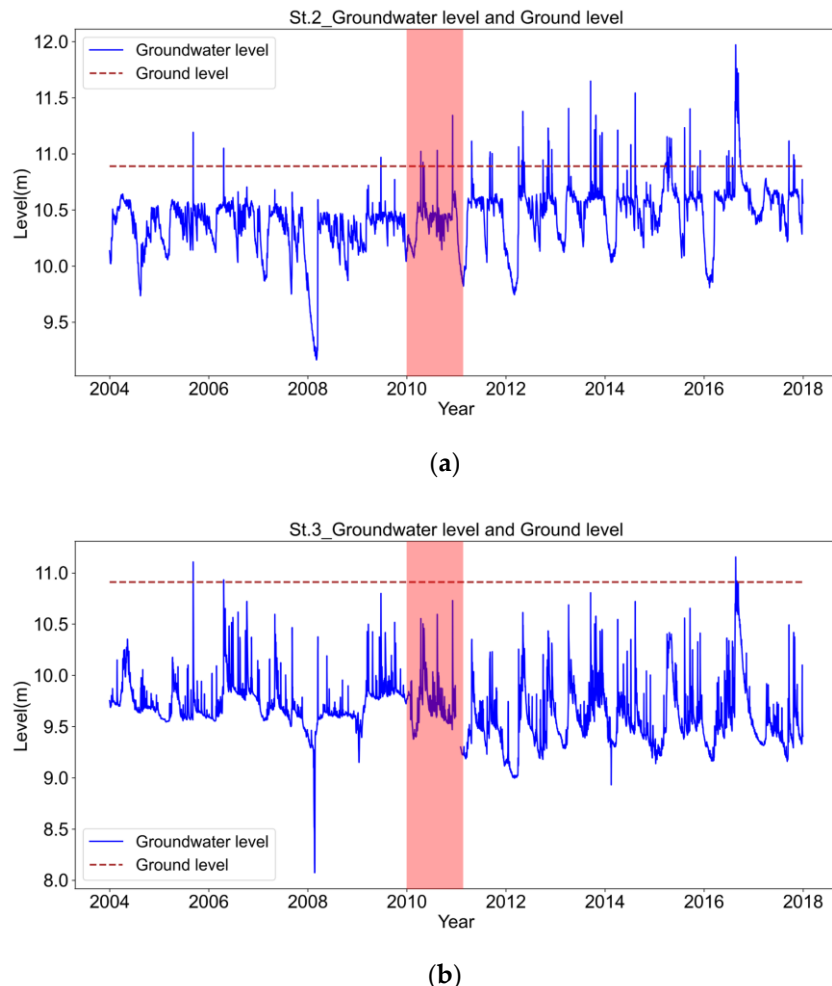
Figure 3 shows the groundwater level observation points in this study. The meandering restored channel of the Kushiro River flows in the south-western direction in Figure 3. There are five observation points, including two upstream, across the meandering restored channel (Sts.1 and 2); one downstream next to the meandering channel (St.3); one between the old straight channel and the meandering channel (St.4); and one reference observation point a further 2 km downstream of St.4 where grassland wetlands are preserved (St.5(ref.): “(ref.)” means the abbreviation of the “reference” point). The former straight channel flowed north of St.2 and St.4, and the remains of the straight channel can be seen faintly in Figure 3.



**Figure 3.** Locations of observation points in the study site of Kushiro Wetland. Source: modified from the image in Google Earth Engine [56].

Figure 4 shows the time series of groundwater levels upstream at St.2 and downstream at St.3. Figure 4 indicates that the amplitude of the groundwater level fluctuations increased after the restoration, and the frequency and intensity of spike-like high-frequency fluctuations also increased. In addition, the mean groundwater level at St.2 upstream became higher after the restoration. It should be noted that a period of significant and

specific decline in groundwater levels was observed in 2008. The Kushiro Wetland usually experiences snowfall from December to the following March during the winter season, and the amount of snowfall affects the groundwater level. The significant drop in the groundwater level in 2008 could be due to the low snowfall in the previous year.



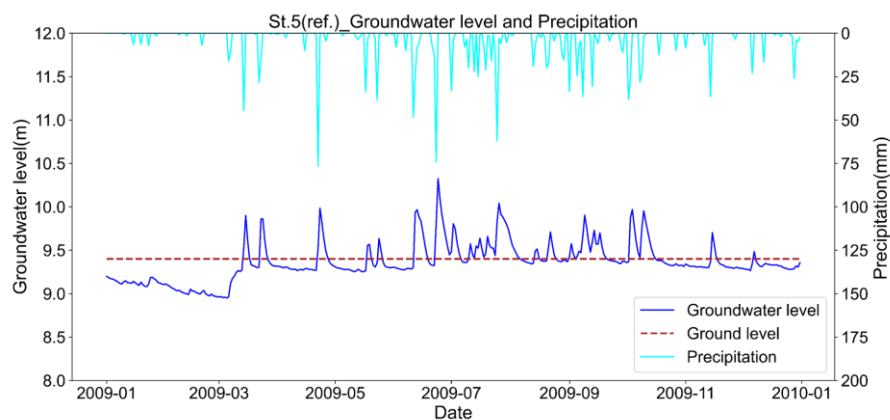
**Figure 4.** Groundwater level time series at observation points in the study site of Kushiro Wetland from 2004 to 2018: (a) St.2; (b) St.3. The red background color indicates the period of the channel restoration.

Figure 5 shows the time series of groundwater levels and rainfall in 2009 at the most downstream site, St.5(ref.). This site, which preserves grassland wetland, indicated an increase in the groundwater level of 40–50 cm in March during the snowmelt season. Then, the water table remained almost at ground level until the end of October, subsequently declining in December when snowfall began. Furthermore, the site is characterized by a very high response of the water table to rainfall events. This grassland wetland remains wet from early June, when the rainy season begins, until late autumn in November. The ground elevation at this site is 9.4 m. The mean groundwater level from 2004 to 2017 was 9.27 m (standard deviation: 0.087 m). This suggests that the close distance between the ground surface and the groundwater level is the original state of the wetland.

## 2.2. Data and Instrumentation

This study used six time series to predict groundwater levels in an LSTM model. The data were temperature, sunshine hours, Normalized Difference Vegetation Index (NDVI), precipitation, snow depth, and river discharge. The first three variables are related to evaporation and transpiration, while the other three variables are related to water inflows

from the atmosphere and upstream. These were used as explanatory variables for the LSTM model described in the following section.



**Figure 5.** Time series of groundwater level and precipitation at St.5 (ref.) in 2009.

The groundwater level time series (daily mean) were obtained from the Kushiro Development and Construction Department, Hokkaido Regional Development Bureau, Ministry of Land, Infrastructure, Transport and Tourism. The air temperature (daily mean), sunshine duration (daily daylight hours), precipitation (daily total), and snow depth (daily deepest recorded) were obtained from the official website of the Japan Meteorological Agency [57] at the observatory site of Shibecha, Hokkaido, Japan. The NDVI was obtained from the Google Earth Engine, in which the MODIS (Moderate Resolution Imaging Spectroradiometer) observations within the study site existed as a 250 m mesh centered at about  $43^{\circ}17'59''$  N,  $144^{\circ}36'3''$  E [56]. For the river discharge (daily mean), observation data were used from the Japanese Ministry of Land, Infrastructure, Transport and Tourism's Hydrological and Water Quality Database [54].

The groundwater levels of St.3 were missing from 23 December 2007 to 31 December 2007 (0.4% of the total), and precipitation data were missing on 15 February 2009. A linear completion was performed for these missing data. The NDVI is 23 times per year (once every 16 days). In order to use an explanatory variable that would allow us to understand the seasonal variability of the NDVI, a linear completion series was applied to the NDVI time series.

### 2.3. Deep Learning Model

This study developed a predictive model for groundwater levels using LSTM [58]. LSTM is a deep learning model developed in the 1990s to overcome the problems of Recurrent Neural Networks (RNN) [59,60]. Since 2010, LSTM has rapidly developed and is one of the most important deep learning methods widely employed in natural language processing, including real-time translation [61]. As already shown in Table 1, it has been applied to many groundwater level time series since 2018.

Figure 6 shows the flowchart of the LSTM structure used in this study. The input layer was exposed to the six explanatory variables measured on three subsequent days to obtain a groundwater level for the following day.

The right-hand side of Figure 6 shows the LSTM model detail used in this study. In addition to two LSTM layers, the model included Dropout, Dense, and Flatten layers with a basic unit count of 128. The activation function used in the LSTM layers was the hyperbolic tangent tanh. A dropout layer with a ratio of 0.2 was added behind each LSTM layer. The optimization function was set to the Adaptive moment (Adam). The maximum number of epochs was set to 100, and early stopping was used as a countermeasure against overfitting. The learning rate was initially set at 0.001 and multiplied by 0.1 every 10 epochs. The LSTM model was implemented in Python [62] v3.8.10, using TensorFlow [63] v2.30,

scikit-learn [64] v0.24.2, Pandas [65] v1.2.4, NumPy [66] v1.19.2, and Keras [67] v2.4.3, which are all open-source libraries.

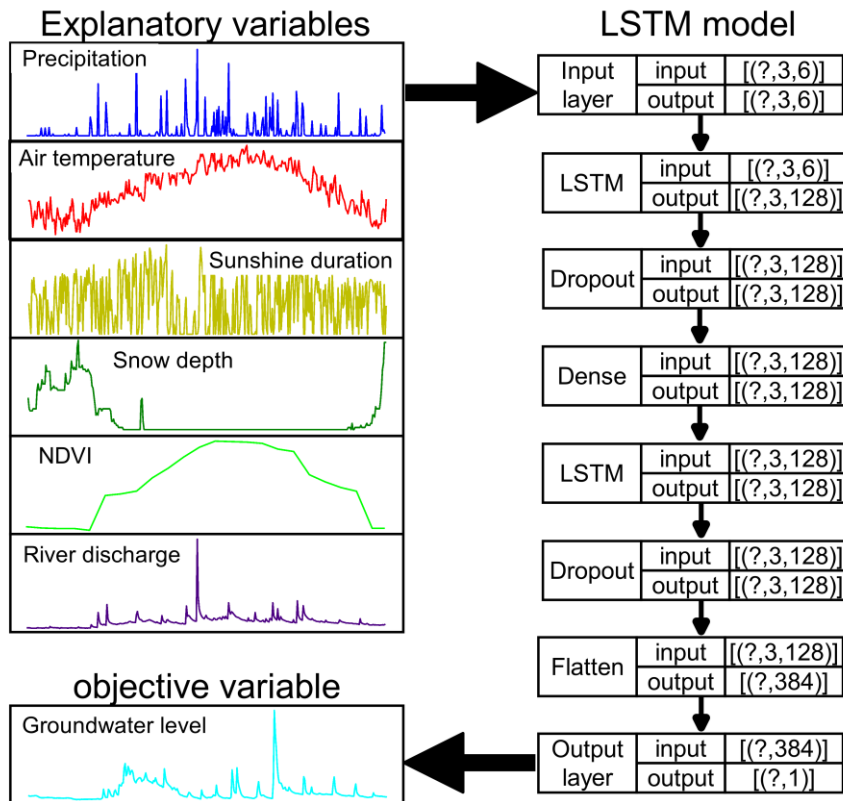


**Figure 6.** The LSTM structure with six explanatory variables for groundwater level prediction. “?” in the right-hand subfigure represents the number of the learning data.

#### 2.4. Steps of the Assessment

##### 2.4.1. Data Division for Pre- and Post-Restoration and the LSTM Evaluation Index

In this study, to evaluate the nature restoration project before and after the meandering stream channel restoration, the decadal data between 2004 and 2017 were divided into two periods, pre- and post-restoration, creating a prediction model for each. The same data length was used for training pre- and post-restoration to eliminate differences in prediction accuracy caused by differences in data volume. Pre-restoration, the learning period was set from 2004 to 2008, with 2009 as the prediction period. Conversely, for post-restoration, the learning period was set from 2012 to 2016, with 2017 as the prediction period.

The root mean square error (RMSE) between the observed and predicted values was used to assess the LSTM model's accuracy. The definition of RMSE is given in Equation (1):

$$RMSE = \sqrt{\frac{1}{N} \sum_{i=1}^N (\hat{y}_i - y_i)^2}, \quad (1)$$

where  $\hat{y}_i$  is the groundwater level predicted by the LSTM model in length, while  $y_i$  is the observed value of the groundwater level.  $N$  is the total number of samples.

##### 2.4.2. Evaluation of the Meandering Stream Channel Restoration

Two LSTM models, before and after the meandering channel restoration, were trained to predict groundwater level fluctuations for each period. These two LSTM models were both applied for the eight years after restoration (2012–2019) with the corresponding observation data of the six explanatory variables. The relative effect of the meandering

channel restoration on groundwater levels was then evaluated by comparing the LSTM results in terms of short- and long-term aspects, as explained in the following.

A short-term perspective analyzes the frequency of groundwater level responses to rainfall. In the grassland wetland time series shown in Figure 5, the groundwater level indicated a high response to rainfall. This study focused on this response: a stepwise frequency analysis was conducted on the groundwater level response for the number of days above the 0.25 m increment threshold for two LSTM predictions, one before restoration and the other after restoration. The increase in frequency was used here as an indicator of the restoration effect of the short-term hydrological characteristics in groundwater levels after the meandering stream channel restoration.

For a long-term perspective, groundwater levels from April to November, excluding the snow season, were compared before and after the restoration. The equation used for evaluation is Equation (2):

$$\Delta\hat{y} = \frac{1}{N} \sum_{i=1}^N (\hat{y}_{i\_a} - \hat{y}_{i\_b}), \quad (2)$$

where  $N$  is the total sample number of groundwater level data for each year after the channel restoration (2012–2018);  $\hat{y}_{i\_a}$  and  $\hat{y}_{i\_b}$  are the predicted groundwater levels (m) on day  $i$  using the LSTM models of after  $_a$  and before  $_b$  the restoration, respectively; and  $\Delta\hat{y}$  is the mean of  $\hat{y}_{i\_a} - \hat{y}_{i\_b}$  in each year of the post-restoration period. Here, a positive  $\Delta\hat{y}$  represents an increase in the mean groundwater level due to the meandering channel restoration, while a negative  $\Delta\hat{y}$  indicates a decrease in the mean groundwater level.

#### 2.4.3. Importance Analysis of the LSTM Explanatory Variables

This study used an applied version of wrapper methods, conventionally used in machine learning [68,69], to analyze the relative importance of explanatory variables in LSTM models (hereafter referred to as AWM for the abbreviation of the applied wrapper method). Conventional wrapper methods attempted to use refining explanatory variables in machine learning. The AWM was used to evaluate the importance of explanatory variables for the LSTM model. In AWM, the truncation of the explanatory variable with a maximum accuracy decline was decided to lead to the most important variable for the LSTM model.

Figure 7 shows a flowchart of AWM. In the AWM procedure, at first, an LSTM model with an explanatory variable truncation was trained with the same hyperparameters as the original LSTM model with all explanatory variables. Then, Equation (3) calculated the relative deviation  $X$  between the RMSEs with observed data in the truncated and original LSTM models. The larger the relative deviation  $X$  between the two models, the higher the importance of the truncated explanatory variable would be expected for the LSTM model:

$$X = \frac{RMSE_{n-1} - RMSE_n}{RMSE_n} \times 100, \quad (3)$$

where  $RMSE_{n-1}$  is the RMSE between observed values and those predicted by the truncated LSTM in  $n - 1$  explanatory variables;  $RMSE_n$  is the RMSE between the observed values and those predicted by the original LSTM in  $n$  explanatory variables; and  $X$  is the relative deviation between  $RMSE_{n-1}$  and  $RMSE_n$ . In recent years, explainable artificial intelligence (XAI) [70] has improved the interpretability of black box deep learning. Importance was able to be determined by applying XAI to LSTM [71]. XAI was not used in this study but will be the topic of future research.

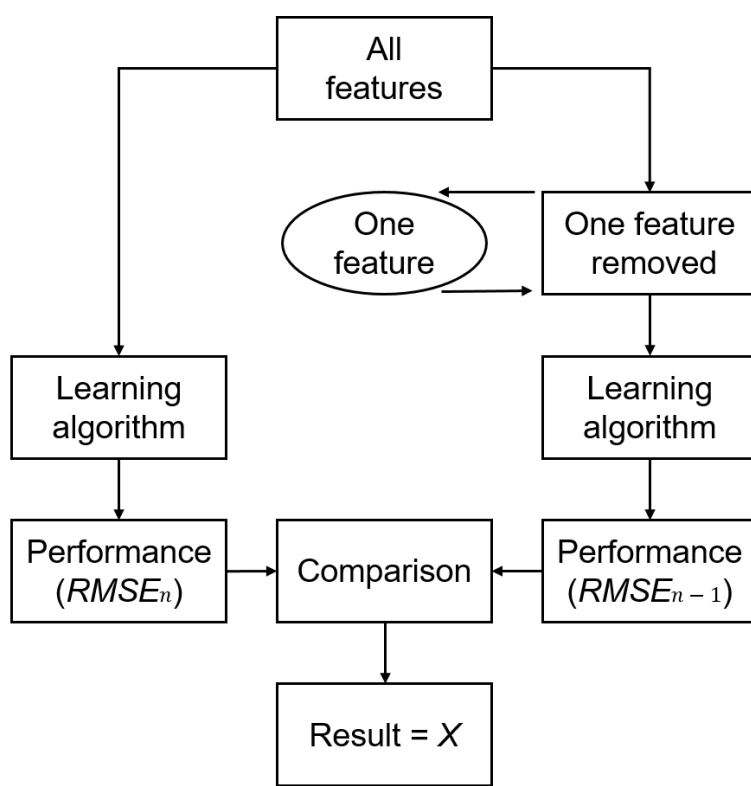


**Figure 7.** The flowchart of the applied wrapper method (AWM) for the importance analysis of explanatory variables in the LSTM model.

### 3. Results

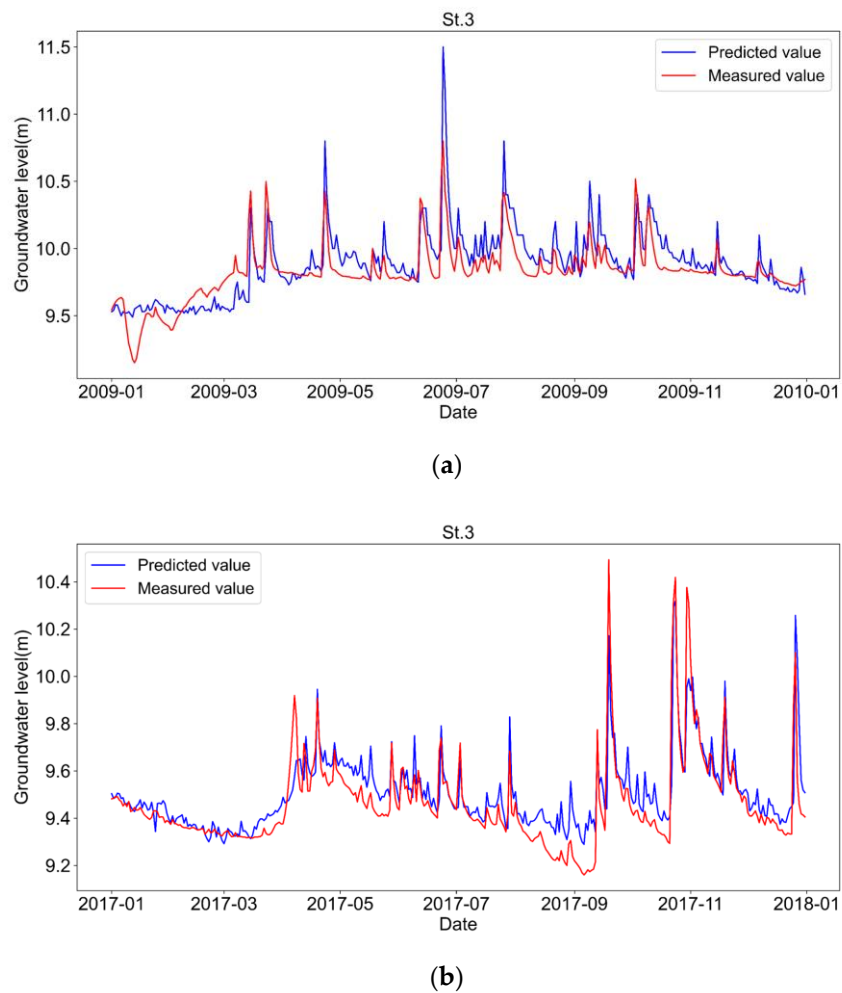
#### 3.1. LSTM Model Accuracy for Groundwater Level Prediction

Figure 8 shows the observed groundwater levels over time and those predicted by LSTM at St.3 in 2009 and 2017, respectively. As noted in Section 2.4, the years 2009 and 2017 were the prediction periods that the two LSTM models learned for the pre- and post-restoration periods. The RMSEs were 0.162 m before the restoration and 0.116 m after the restoration. Figure 8 indicates that the LSTM models can predict groundwater level fluctuation characteristics of the observed values, including their sudden increases due to rainfall. The main reason for the prediction error would be during recessions, in which the predicted groundwater level decreased more slowly than the observed one immediately after rainfall.

Table 2 summarizes the RMSEs for Sts.1–4. The RMSEs ranged between 0.082 and 0.162 m. As shown in Figure 8, the LSTM model accurately predicted the groundwater level response to rainfall. These results strongly support that the prediction error of the LSTM model is sufficiently small. Therefore, we confirmed that the LSTM model has sufficient accuracy to evaluate the meandering stream channel restoration effect in this study.

**Table 2.** RMSEs before and after the meandering stream channel restoration.

Observation Point	RMSE before Restoration in 2009 (m)	RMSE after Restoration in 2017 (m)
St.1	0.082	0.134
St.2	0.094	0.139
St.3	0.162	0.116
St.4	0.161	0.136



**Figure 8.** Time series of groundwater levels at St.3 from both the LSTM prediction and field observation: (a) Before the meandering stream channel restoration in 2009. (b) After the meandering stream channel restoration in 2017.

### 3.2. Evaluation of the Meandering Stream Channel Restoration

Figure 9 shows the typical results of the short-term evaluation. It indicates the frequency analysis of groundwater level responses to rainfall for St.2 (upstream) in 2014 and St.4 (downstream) in 2016 using the two LSTM models for pre- and post-restoration. The results for all the periods and stations are presented below in Table 3. Figure 9 indicates that the frequency of groundwater level response to rainfall has increased after the restoration of the old meandering stream channel at both observation stations. In particular, at the upstream station St.2, the frequency of groundwater level fluctuations increased significantly at the small amplitude of +0.25 m. On the other hand, as shown in Figure 9b, the fluctuation of the groundwater level above +1.00 m at St.4 decreased in frequency after the restoration.

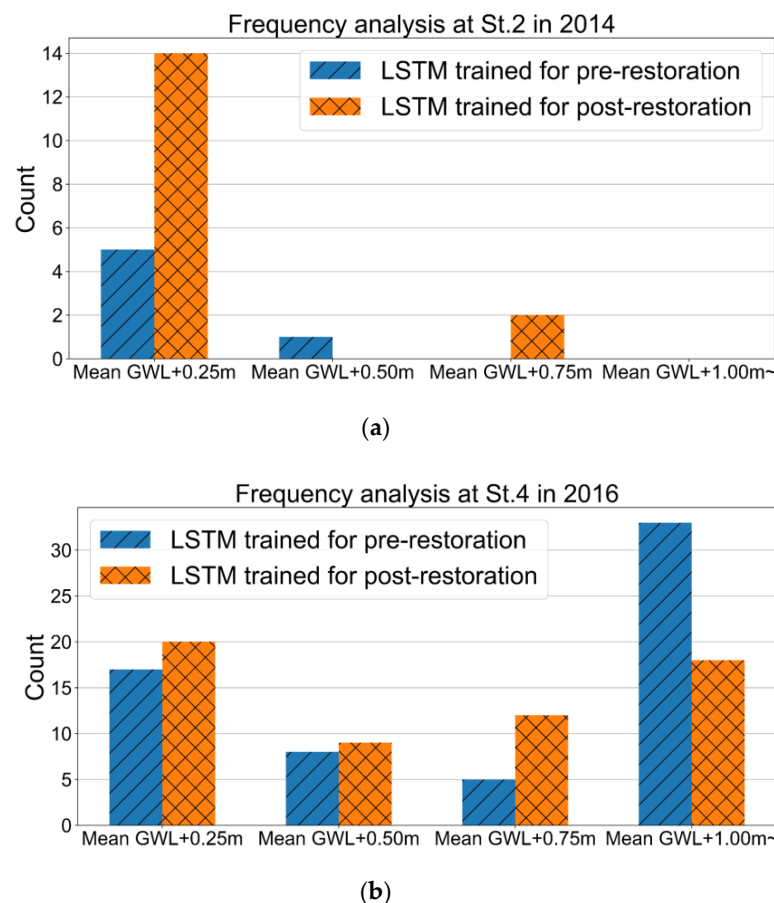


**Figure 9.** Frequency analysis of groundwater level response to rainfall using the LSTM models: (a) Observation point St.2, the upstream side, in 2014. (b) Observation point St.4, the downstream side, in 2016.

**Table 3.** Annual mean frequency of groundwater level response to rainfall: (a) Before the meandering stream channel restoration. (b) After the meandering stream channel restoration.

(a)				
Counts	St.1	St.2	St.3	St.4
Mean GWL +0.25 m	13.4	12.2	20.0	29.3
Mean GWL +0.50 m	0.667	0.667	7.11	11.0
Mean GWL +0.75 m	0	0.333	2.00	4.44
Mean GWL +1.00 m~	0	0	4.00	6.11
Total counts	14.1	13.2	33	50.9
(b)				
Counts	St.1	St.2	St.3	St.4
Mean GWL +0.25 m	20.1	22.4	29.2	34.0
Mean GWL +0.50 m	3.11	3.11	8.89	11.3
Mean GWL +0.75 m	1.78	1.22	5.22	3.89
Mean GWL +1.00 m~	0.444	0.111	2.78	3.33
Total counts	25.4	26.9	46.1	52.6

Note: GWL: Groundwater level.

Table 3 summarizes the annual mean frequency of groundwater level response to rainfall at all stations before and after the restoration. The frequency ratio increased at Sts. 1–4 by 1.80, 2.04, 1.39, and 1.03, respectively. Therefore, the groundwater level response to rainfall has become more frequent after the restoration at all the observation points. In particular, the upstream side indicated more significant increases in frequency compared to the downstream side.

Figure 10 shows the boxplots of the mean groundwater level change  $\Delta\hat{y}$  before and after the restoration at the observation points St.1 to 4 from April to November, excluding the snow season. The median values of  $\Delta\hat{y}$  at the upstream observation points (St.1 and St.2) were 0.040 m and 0.145 m, respectively, and at the downstream observation points (St.3 and St.4), these values were  $-0.117$  m and  $-0.208$  m, respectively. This indicated that the meandering stream channel restoration caused increases in the groundwater level upstream and decreases downstream. In addition, it resulted in a more significant rise in the groundwater level at St.2, located far from the restored meandering stream channel. These results reveal that the groundwater hydrological characteristics from a long-term perspective show a trend toward a wetland environment upstream but toward a drying trend downstream. Furthermore, the mean groundwater level at observation point St.5(ref.), shown in Figure 5, remains at ground level. In contrast, the groundwater levels do not reach ground level at all at the observation points St.1 to 4 in the meandering stream channel restoration area.

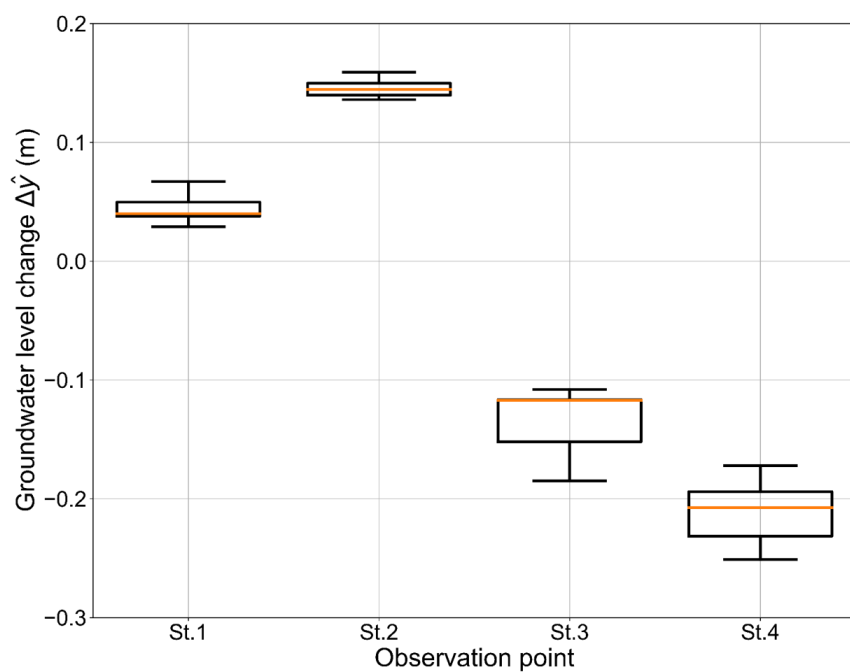


**Figure 10.** Boxplots of groundwater level changes before and after the meandering stream channel restoration at the observation points Sts.1–4.

### 3.3. Importance Analysis for the LSTM Model Explanatory Variables

Figure 11 shows the results of applying AWM to the LSTM model before and after the restoration to analyze the importance of explanatory variables. The vertical axis of Figure 11 is the relative deviation  $X$  calculated by Equation (3). As a result, although there were variations between observation points, the relative deviations  $X$  of river discharge and precipitation were more significant than those of other explanatory variables, regardless of whether the meandering stream channel was restored. This clearly indicates that river discharge and precipitation significantly affect the fluctuation of groundwater level in the LSTM model. These are hydrological quantities strongly related to the changes in mean groundwater levels in the short-term and long-term perspectives described above. In

addition, even if the observation point was close to the river channel, the importance of the river discharge was not necessarily high.

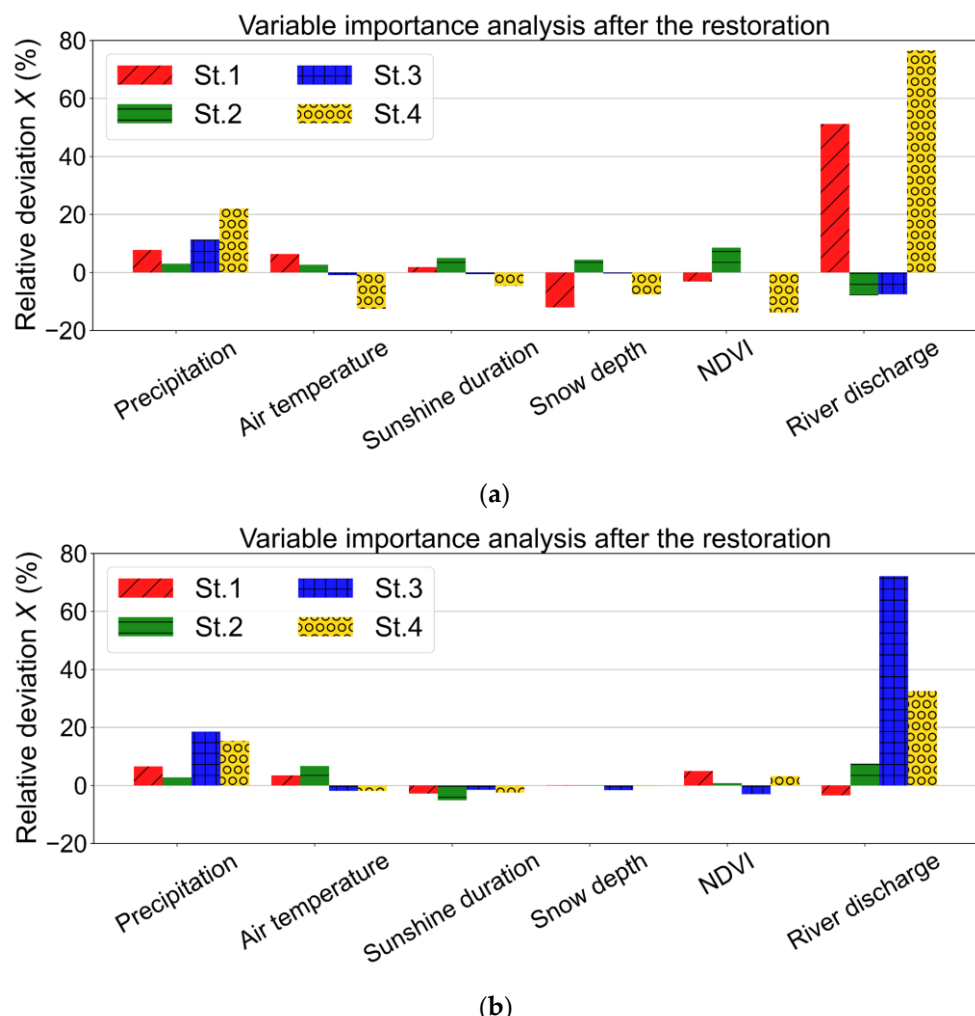


**Figure 11.** Importance analysis of the explanatory variables in the LSTM models by AWM: (a) Before the meandering stream channel restoration. (b) After the meandering stream channel restoration.

#### 4. Discussion

##### 4.1. Advantages and Limitations of the LSTM Model in This Study

In this study, an LSTM model was trained for each of the pre- and post-restoration periods when the hydrological and geological characteristics changed due to the river channel's restoration. The LSTM model was able to quantitatively predict the groundwater level's response to rainfall as well as changes in the annual mean groundwater level before and after the restoration of the meandering stream channel. The use of LSTM allowed an evaluation of the effect of nature restoration on the hydrological characteristics of groundwater. The time series data used for the learning of the LSTM model were analyzed for abundant rainfall events that occur frequently as well as the mean groundwater level that exists as a basic trend. In other words, the LSTM model in this study was able to learn those abundant data features as a black box model. So far, the assessment of hydrological properties in wetland environments has mainly used complex physical-process-based models [22–25]. On the other hand, the LSTM model in this study is data-driven, making it an excellent alternative method that can learn the hydrological and geological characteristics in different environments without detailed geophysical settings.

As for the model's limitations, the LSTM model in this study could not successfully predict the large drop in groundwater level in spring 2008, as shown in Figure 4. This large

drop in the groundwater level was due to the lack of snowfall in the previous winter. This was a low-frequency phenomenon only occurring in that year in the learning data before the restoration. Snow depth was also included as an explanatory variable in the LSTM model, but predicting phenomena that rarely occur in the learning dataset was challenging. In this study, since we focused on the rainfall response and the annual mean groundwater level, it was sufficient to set the learning data periods before and after the restoration to five years. However, in general, deep learning could be expected to improve prediction accuracy with big data [45]. Furthermore, it has been reported that at least 10 to 12 years of consecutive data are required for accurate monthly mean groundwater level prediction using machine learning [72]. Therefore, to use a data-driven deep learning model when the amount of data is limited, such as the LSTM model in this study, it should be essential to apply the model based on the characteristics of the dataset and the learning model.

#### 4.2. Restoration of Hydrological Processes and Wetland Ecosystems in the Kushiro Wetland

The LSTM model analysis in this study indicated that groundwater hydrological characteristics, such as rainfall response and mean groundwater level, tended to recover to the previous state before 1984 after the meandering stream channel was restored. In particular, the recovery trend was remarkable on the upstream side of the study site. However, even though the natural restoration project restored the flow path to its previous meandering state, alder trees continue to flourish in the area, and the grassland wetland has not yet been restored, even after one decade. This issue might be due to increased local evapotranspiration caused by the trees, having created a gap in groundwater level recovery. Cases where the hydrological environment has recovered but the wetlands have not been restored have also been reported in the Scott Starling Nature Sanctuary in the United States [73] and the Rhone River in France [74].

In the Kushiro Wetland, the sedge family forms herbaceous clumps (called “Yachibouzu” in Japanese) on which alder trees can grow, as shown in Figure 12. This situation makes it possible for alder trees to survive in a unique wetland environment that experiences snowfall in winter and snowmelt in spring. The growing environment created by Yachibouzu could be one of the reasons why it is difficult to return to the grassland wetland environment once woody plants have invaded it.

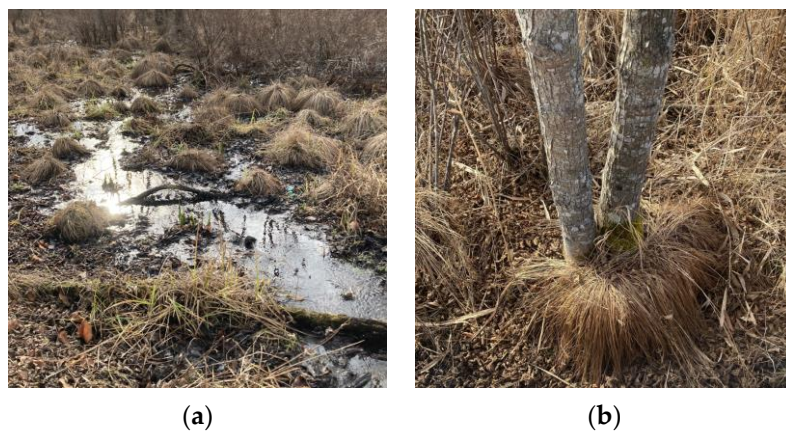


**Figure 12.** The herbaceous clumps of the sedge family in the Kushiro Wetland (“Yachibouzu” in Japanese): (a) Without alder trees. (b) With alder trees.

In addition, it has been reported that peat soil properties are essential for the natural restoration of peat swamps [75], and complete restoration of peatlands is impossible [76]. Based on these findings, restoring groundwater characteristics alone would not be sufficient to restore peat grassland wetlands such as the Kushiro Wetland. There is also a report that a combination of stream channel improvement and tree cutting could be effective in swamps in Sweden [77]. Even in the Kushiro Wetland, under the current situation where

the meandering stream channel restoration has shown a trend toward the recovery of hydrological conditions, a further restoration approach would be necessary, e.g., combining soil improvement and the removal of woody plants.

#### 4.3. Future Model Development

The LSTM model in this study was a simple groundwater level prediction model that focused on rainfall responses and mean groundwater level changes. Applying it before and after the meandering stream channel's restoration made it possible to evaluate the hydrological process part of the restoration. On the other hand, the LSTM model could not reproduce the low-frequency events in the dataset, such as the drop in groundwater level caused by the small amount of snowfall described above. In general, observation data obtained from nature restoration projects are limited. Therefore, to improve the prediction accuracy of the model, it would be essential to pre- and post-process the features inherent in the dataset [27,78–80]. New metaheuristic algorithms [81] would be useful for machine learning modeling with limited datasets. In addition, as mentioned in the section on the importance analysis of explanatory variables, the LSTM model of this study would be insufficient to consider the relationship between groundwater level fluctuations and topography/soil. Therefore, it would also be important to use machine learning models that can express their spatial distribution characteristics [42] and to develop hybrid data-driven deep learning models that combine the outputs of physical process models [16].

### 5. Conclusions

In this study, LSTM models learned groundwater level characteristics pre- and post-restoration of a meandering river channel and analyzed how hydrological and geological characteristics changed due to the channel's restoration. This study chose the precipitation, air temperature, sunshine duration, snow depth, NDVI, and river discharge as the explanatory variables of the LSTM model, which were easily available through the public domain. The trained LSTM models achieved high performance, with prediction RMSEs for the groundwater levels that were within 0.162 m at all the observation points. The analysis of the simple LSTM models clarified that the meandering stream channel restoration regained hydrological processes in groundwater levels, i.e., their rainfall responses and mean groundwater levels. In particular, the restoration tendency was remarkable at the observation points on the upstream side. Furthermore, the variable importance analysis of the explanatory variables in the LSTM model showed that river discharge and precipitation significantly contributed to groundwater level recovery in the Kushiro Wetland.

The LSTM model in this study is data-driven, making it an excellent alternative method that could learn the hydrological and geological characteristics in different environments without detailed geophysical settings. Subsequently, when the amount of data is limited, as in this research, it would be essential to apply hybrid models based on the dataset features and the machine learning characteristics.

**Author Contributions:** Conceptualization, H.M.; methodology, T.Y. and H.M.; software, T.Y.; validation, T.Y. and T.O.; formal analysis, T.Y.; investigation, T.Y. and T.O.; resources, T.O.; writing—original draft preparation, T.Y.; writing—review and editing, H.M. and T.O.; visualization, T.Y.; supervision, H.M.; project administration, H.M. and T.O.; funding acquisition, H.M. All authors have read and agreed to the published version of the manuscript.

**Funding:** Partial support from the Japan Society for the Promotion of Science (JSPS) KAKENHI through a Grant-in-Aid for Scientific Research (No. JP20H02261) and from the River Fund of the River Foundation, Japan (No. 2020-5211-045), is gratefully acknowledged.

**Data Availability Statement:** The data presented in this study are available from information in the reference list of this article. The groundwater level observation data in this study are available via the corresponding author upon a reasonable request.

**Acknowledgments:** The groundwater level observation data used in this study were provided by the Kushiro Development and Construction Department, Hokkaido Regional Development Bureau, Ministry of Land, Infrastructure, Transport and Tourism. The authors are grateful for their support and data provision. The authors also thank the three anonymous reviewers for their useful comments.

**Conflicts of Interest:** The authors declare no conflict of interest.

## References

1. Costanza, R.; d’Arge, R.; de Groot, R.; Farber, S.; Grasso, M.; Hannon, B.; Limburg, K.; Naeem, S.; O’Neill, R.V.; Paruelo, J.; et al. The value of the world’s ecosystem services and natural capital. *Nature* **1997**, *387*, 253–260. [[CrossRef](#)]
2. Verhoeven, J.; Setter, T. Agricultural use of wetlands: Opportunities and limitations. *Ann. Bot.* **2009**, *105*, 155–163. [[CrossRef](#)]
3. Hassan, R.; Scholes, R.; Ash, N. *Ecosystems and Human Well-Being: Current State and Trends*; Island Press: Washington, DC, USA, 2005.
4. Mitsch, W.J.; Bernal, B.; Hernandez, M.E. Ecosystem services of wetlands. *Int. J. Biodivers. Sci. Ecosyst. Serv. Manag.* **2015**, *11*, 1–4. [[CrossRef](#)]
5. Gardner, R.C.; Finlayson, M. *Global Wetland Outlook: State of the World’s Wetlands and Their Services to People 2018*; Secretariat of the Ramsar Convention: Gland, Switzerland, 2018.
6. Weise, K.; Höfer, R.; Franke, J.; Guelmami, A.; Simonson, W.; Muro, J.; O’Connor, B.; Strauch, A.; Flink, S.; Eberle, J.; et al. Wetland extent tools for SDG 6.6.1 reporting from the Satellite-based Wetland Observation Service (SWOS). *Remote Sens. Environ.* **2020**, *247*, 111892. [[CrossRef](#)]
7. Zedler, J.B. Progress in wetland restoration ecology. *Trends Ecol. Evol.* **2000**, *15*, 402–407. [[CrossRef](#)]
8. Harvey, M.C.; Hare, D.K.; Hackman, A.; Davenport, G.; Haynes, A.B.; Helton, A.; Lane, J.W.; Briggs, M.A. Evaluation of Stream and Wetland Restoration Using UAS-Based Thermal Infrared Mapping. *Water* **2019**, *11*, 1568. [[CrossRef](#)]
9. Hunt, R.J.; Walker, J.F.; Krabbenhoft, D.P. Characterizing hydrology and the importance of ground-water discharge in natural and constructed wetlands. *Wetlands* **1999**, *19*, 458–472. [[CrossRef](#)]
10. Acreman, M.C.; Fisher, J.; Stratford, C.J.; Mould, D.J.; Mountford, J.O. Hydrological science and wetland restoration: Some case studies from Europe. *Hydrol. Earth Syst. Sci.* **2007**, *11*, 158–169. [[CrossRef](#)]
11. Banaszuk, P.; Kamocki, A. Effects of climatic fluctuations and land-use changes on the hydrology of temperate fluvioogenous mire. *Ecol. Eng.* **2008**, *32*, 133–146. [[CrossRef](#)]
12. Grodzka-Łukaszewska, M.; Simicyn, G.; Grygoruk, M.; Mirosław-Świątek, D.; Kardel, I.; Okruszko, T. The role of the river in the functioning of marginal fen: A case study from the Biebrza Wetlands. *PeerJ* **2022**, *10*, e13418. [[CrossRef](#)]
13. Dorau, K.; Gelhausen, H.; Esplör, D.; Mansfeldt, T. Wetland restoration management under the aspect of climate change at a mesotrophic fen in Northern Germany. *Ecol. Eng.* **2015**, *84*, 84–91. [[CrossRef](#)]
14. Nakamura, K.; Tockner, K.; Amano, K. River and Wetland Restoration: Lessons from Japan. *BioScience* **2006**, *56*, 419–429. [[CrossRef](#)]
15. Nakamura, F.; Ishiyama, N.; Sueyoshi, M.; Negishi, J.N.; Akasaka, T. The Significance of Meander Restoration for the Hydrogeomorphology and Recovery of Wetland Organisms in the Kushiro River, a Lowland River in Japan. *Restor. Ecol.* **2014**, *22*, 544–554. [[CrossRef](#)]
16. Nakayama, T. Feedback and regime shift of mire ecosystem in northern Japan. *Hydrol. Process.* **2012**, *26*, 2455–2469. [[CrossRef](#)]
17. Johansen, O.M.; Andersen, D.K.; Ejrnæs, R.; Pedersen, M.L. Relations between vegetation and water level in groundwater dependent terrestrial ecosystems (GWDTEs). *Limnologica* **2018**, *68*, 130–141. [[CrossRef](#)]
18. Toogood, S.E.; Joyce, C.B. Effects of raised water levels on wet grassland plant communities. *Appl. Veg. Sci.* **2009**, *12*, 283–294. [[CrossRef](#)]
19. Hammersmark, C.T.; Rains, M.C.; Wickland, A.C.; Mount, J.F. Vegetation and water-table relationships in a hydrologically restored riparian meadow. *Wetlands* **2009**, *29*, 785–797. [[CrossRef](#)]
20. Kopeć, D.; Michalska-Hejduk, D.; Krogulec, E. The relationship between vegetation and groundwater levels as an indicator of spontaneous wetland restoration. *Ecol. Eng.* **2013**, *57*, 242–251. [[CrossRef](#)]
21. Orellana, E.; Verma, P.; Loheide II, S.P.; Daly, E. Monitoring and modeling water-vegetation interactions in groundwater-dependent ecosystems. *Rev. Geophys.* **2012**, *50*, RG3003. [[CrossRef](#)]
22. Boswell, J.S.; Olyphant, G.A. Modeling the hydrologic response of groundwater dominated wetlands to transient boundary conditions: Implications for wetland restoration. *J. Hydrol.* **2007**, *332*, 467–476. [[CrossRef](#)]
23. Hammersmark, C.T.; Rains, M.C.; Mount, J.F. Quantifying the hydrological effects of stream restoration in a montane meadow, northern California, USA. *River Res. Appl.* **2008**, *24*, 735–753. [[CrossRef](#)]
24. Loheide, S.P.; Booth, E.G. Effects of changing channel morphology on vegetation, groundwater, and soil moisture regimes in groundwater-dependent ecosystems. *Geomorphology* **2011**, *126*, 364–376. [[CrossRef](#)]
25. Montalto, F.A.; Parlange, J.-Y.; Steenhuis, T.S. A simple model for predicting water table fluctuations in a tidal marsh. *Water Resour. Res.* **2007**, *43*, W03439. [[CrossRef](#)]
26. Gu, H.; Xu, Y.-P.; Ma, D.; Xie, J.; Liu, L.; Bai, Z. A surrogate model for the Variable Infiltration Capacity model using deep learning artificial neural network. *J. Hydrol.* **2020**, *588*, 125019. [[CrossRef](#)]

27. Liu, W.; Yu, H.; Yang, L.; Yin, Z.; Zhu, M.; Wen, X. Deep Learning-Based Predictive Framework for Groundwater Level Forecast in Arid Irrigated Areas. *Water* **2021**, *13*, 2558. [[CrossRef](#)]
28. Arel, I.; Rose, D.C.; Karnowski, T.P. Deep Machine Learning—A New Frontier in Artificial Intelligence Research [Research Frontier]. *IEEE Comput. Intell. Mag.* **2010**, *5*, 13–18. [[CrossRef](#)]
29. LeCun, Y.; Bengio, Y.; Hinton, G. Deep learning. *Nature* **2015**, *521*, 436–444. [[CrossRef](#)] [[PubMed](#)]
30. Mohapatra, J.B.; Jha, P.; Jha, M.K.; Biswal, S. Efficacy of machine learning techniques in predicting groundwater fluctuations in agro-ecological zones of India. *Sci. Total Environ.* **2021**, *785*, 147319. [[CrossRef](#)]
31. Han, K.; Wang, Y. A review of artificial neural network techniques for environmental issues prediction. *J Anal Calorim* **2021**, *145*, 2191–2207. [[CrossRef](#)]
32. Shen, C. A Transdisciplinary Review of Deep Learning Research and Its Relevance for Water Resources Scientists. *Water Resour. Res.* **2018**, *54*, 8558–8593. [[CrossRef](#)]
33. Tahmasebi, P.; Kamrava, S.; Bai, T.; Sahimi, M. Machine learning in geo- and environmental sciences: From small to large scale. *Adv. Water Resour.* **2020**, *142*, 103619. [[CrossRef](#)]
34. Tao, H.; Hameed, M.M.; Marhoon, H.A.; Zounemat-Kermani, M.; Heddam, S.; Kim, S.; Sulaiman, S.O.; Tan, M.L.; Sa’adi, Z.; Mehr, A.D.; et al. Groundwater level prediction using machine learning models: A comprehensive review. *Neurocomputing* **2022**, *489*, 271–308. [[CrossRef](#)]
35. Zhang, J.; Zhu, Y.; Zhang, X.; Ye, M.; Yang, J. Developing a Long Short-Term Memory (LSTM) based model for predicting water table depth in agricultural areas. *J. Hydrol.* **2018**, *561*, 918–929. [[CrossRef](#)]
36. Jeong, J.; Park, E. Comparative applications of data-driven models representing water table fluctuations. *J. Hydrol.* **2019**, *572*, 261–273. [[CrossRef](#)]
37. Bowes, B.D.; Sadler, J.M.; Morsy, M.M.; Behl, M.; Goodall, J.L. Forecasting Groundwater Table in a Flood Prone Coastal City with Long Short-term Memory and Recurrent Neural Networks. *Water* **2019**, *11*, 1098. [[CrossRef](#)]
38. Huang, X.; Gao, L.; Crosbie, R.S.; Zhang, N.; Fu, G.; Doble, R. Groundwater Recharge Prediction Using Linear Regression, Multi-Layer Perception Network, and Deep Learning. *Water* **2019**, *11*, 1879. [[CrossRef](#)]
39. Kim, G.-B.; Hwang, C.-I.; Choi, M.-R. PCA-based multivariate LSTM model for predicting natural groundwater level variations in a time-series record affected by anthropogenic factors. *Environ. Earth Sci.* **2021**, *80*, 657. [[CrossRef](#)]
40. Liang, Z.; Liu, Y.; Hu, H.; Li, H.; Ma, Y.; Khan, M.Y.A. Combined Wavelet Transform with Long Short-Term Memory Neural Network for Water Table Depth Prediction in Baoding City, North China Plain. *Front. Environ. Sci.* **2021**, *9*, 780434. [[CrossRef](#)]
41. He, L.; Hou, M.; Chen, S.; Zhang, J.; Chen, J.; Qi, H. Construction of a spatio-temporal coupling model for groundwater level prediction: A case study of Changwu area, Yangtze River Delta region of China. *Water Supply* **2021**, *21*, 3790–3809. [[CrossRef](#)]
42. Guo, F.; Yang, J.; Li, H.; Li, G.; Zhang, Z. A ConvLSTM Conjunction Model for Groundwater Level Forecasting in a Karst Aquifer Considering Connectivity Characteristics. *Water* **2021**, *13*, 2759. [[CrossRef](#)]
43. Dey, S.; Dey, A.K.; Mall, R.K. Long Short-Term Memory Neural Network (LSTM-NN) for Aquifer Level Time Series Forecasting Using in-Situ Piezo-metric Observations. *Water Resour. Manag.* **2021**, *35*, 3395–3410. [[CrossRef](#)]
44. Ghasemlounia, R.; Gharehbaghi, A.; Ahmadi, F.; Saadatnejadgharahassanlou, H. Developing a novel framework for forecasting groundwater level fluctuations using Bi-directional Long Short-Term Memory (BiLSTM) deep neural network. *Comput. Electron. Agric.* **2021**, *191*, 106568. [[CrossRef](#)]
45. Wunsch, A.; Liesch, T.; Broda, S. Groundwater level forecasting with artificial neural networks: A comparison of long short-term memory (LSTM), convolutional neural networks (CNNs), and non-linear autoregressive networks with exogenous input (NARX). *Hydrol. Earth Syst. Sci.* **2021**, *25*, 1671–1687. [[CrossRef](#)]
46. Ma, Y.; Montzka, C.; Bayat, B.; Kollet, S. Using Long Short-Term Memory networks to connect water table depth anomalies to precipitation anomalies over Europe. *Hydrol. Earth Syst. Sci.* **2021**, *25*, 3555–3575. [[CrossRef](#)]
47. Müller, J.; Park, J.; Sahu, R.; Varadharajan, C.; Arora, B.; Faybishenko, B.; Agarwal, D. Surrogate optimization of deep neural networks for groundwater predictions. *J Glob Optim* **2021**, *81*, 203–231. [[CrossRef](#)]
48. Solgi, R.; Loáiciga, H.A.; Kram, M. Long short-term memory neural network (LSTM-NN) for aquifer level time series forecasting using in-situ piezometric observations. *J. Hydrol.* **2021**, *601*, 126800. [[CrossRef](#)]
49. Hakim, W.L.; Nur, A.S.; Rezaie, F.; Panahi, M.; Lee, C.-W.; Lee, S. Convolutional neural network and long short-term memory algorithms for groundwater potential mapping in Anseong, South Korea. *J. Hydrol. Reg. Stud.* **2022**, *39*, 100990. [[CrossRef](#)]
50. Japan Meteorological Agency Japan Meteorological Agency Web Site. Available online: <https://www.data.jma.go.jp/obd/stats/etrn/> (accessed on 8 March 2023).
51. Kushiro-shitsugen | Ramsar Sites Information Service. Available online: <https://rsis.ramsar.org/ris/205> (accessed on 8 March 2023).
52. Nakayama, T. Factors controlling vegetation succession in Kushiro Mire. *Ecol. Model.* **2008**, *215*, 225–236. [[CrossRef](#)]
53. Nakamura, F.; Sudo, T.; Kameyama, S.; Jitsu, M. Influences of channelization on discharge of suspended sediment and wetland vegetation in Kushiro Marsh, northern Japan. *Geomorphology* **1997**, *18*, 279–289. [[CrossRef](#)]
54. Ministry of Land, Infrastructure, Transport and Tourism, H.Q.D. Ministry of Land, Infrastructure, Transport and Tourism Hydrologic Quality Database. Available online: <http://www1.river.go.jp/> (accessed on 8 March 2023).
55. Geospatial Information Authority of Japan Geospatial Information Authority of Japan. Available online: <https://www.gsi.go.jp/ENGLISH/index.html> (accessed on 8 March 2023).

56. Gorelick, N.; Hancher, M.; Dixon, M.; Ilyushchenko, S.; Thau, D.; Moore, R. Google Earth Engine: Planetary-scale geospatial analysis for everyone. *Remote Sens. Environ.* **2017**, *202*, 18–27. [[CrossRef](#)]
57. Japan Meteorological Agency, W.S. Japan Meteorological Agency Web Site. Available online: <https://www.data.jma.go.jp/gmd/risk/obssl/> (accessed on 8 March 2023).
58. Hochreiter, S.; Schmidhuber, J. Long Short-Term Memory. *Neural Comput.* **1997**, *9*, 1735–1780. [[CrossRef](#)]
59. Informatik, F.; Bengio, Y.; Frasconi, P.; Schmidhuber, J. Gradient Flow in Recurrent Nets: The Difficulty of Learning Long-Term Dependencies. In *A Field Guide to Dynamical Recurrent Neural Networks*; IEEE Press: Piscataway, NJ, USA, 2003.
60. Graves, A.; Schmidhuber, J. Framewise phoneme classification with bidirectional LSTM and other neural network architectures. *Neural Netw.* **2005**, *18*, 602–610. [[CrossRef](#)]
61. Yao, L.; Guan, Y. An Improved LSTM Structure for Natural Language Processing. In Proceedings of the 2018 IEEE International Conference of Safety Produce Informatization (IICSPI), Chongqing, China, 10–12 December 2018; pp. 565–569.
62. Python. Available online: <https://www.python.org/> (accessed on 8 March 2023).
63. TensorFlow. Available online: <https://www.tensorflow.org/> (accessed on 8 March 2023).
64. scikit-learn. Available online: <https://scikit-learn.org/> (accessed on 8 March 2023).
65. Pandas. Available online: <https://pandas.pydata.org/> (accessed on 8 March 2023).
66. NumPy. Available online: <https://numpy.org/> (accessed on 8 March 2023).
67. Keras. Available online: <https://keras.io/> (accessed on 8 March 2023).
68. Rodriguez-Galiano, V.F.; Luque-Espinar, J.A.; Chica-Olmo, M.; Mendes, M.P. Feature selection approaches for predictive modelling of groundwater nitrate pollution: An evaluation of filters, embedded and wrapper methods. *Sci. Total Environ.* **2018**, *624*, 661–672. [[CrossRef](#)]
69. Yang, P.; Liu, W.; Zhou, B.B.; Chawla, S.; Zomaya, A.Y. Ensemble-Based Wrapper Methods for Feature Selection and Class Imbalance Learning. In Proceedings of the Advances in Knowledge Discovery and Data Mining; Pei, J., Tseng, V.S., Cao, L., Motoda, H., Xu, G., Eds.; Springer: Berlin/Heidelberg, Germany, 2013; pp. 544–555.
70. Gunning, D. Explainable Artificial Intelligence (XAI). *Def. Adv. Res. Proj. Agency Web* **2017**, *2*, 1.
71. Adak, A.; Pradhan, B.; Shukla, N.; Alamri, A. Unboxing Deep Learning Model of Food Delivery Service Reviews Using Explainable Artificial Intelligence (XAI) Technique. *Foods* **2022**, *11*, 2019. [[CrossRef](#)]
72. Ahmadi, A.; Olyaei, M.; Heydari, Z.; Emami, M.; Zeynolabedin, A.; Ghomlaghi, A.; Daccache, A.; Fogg, G.E.; Sadegh, M. Groundwater Level Modeling with Machine Learning: A Systematic Review and Meta-Analysis. *Water* **2022**, *14*, 949. [[CrossRef](#)]
73. Vidon, P.; Jacinthe, P.-A.; Liu, X.; Fisher, K.; Baker, M. Hydrobiogeochemical Controls on Riparian Nutrient and Greenhouse Gas Dynamics: 10 Years Post-Restoration. *JAWRA J. Am. Water Resour. Assoc.* **2014**, *50*, 639–652. [[CrossRef](#)]
74. Henry, C.P.; Amoros, C.; Giuliani, Y. Restoration ecology of riverine wetlands: II. An example in a former channel of the Rhône River. *Environ. Manag.* **1995**, *19*, 903–913. [[CrossRef](#)]
75. Erwin, K.L. Wetlands and global climate change: The role of wetland restoration in a changing world. *Wetl. Ecol Manag.* **2008**, *17*, 71. [[CrossRef](#)]
76. Klimkowska, A.; Van Diggelen, R.; Grootjans, A.P.; Kotowski, W. Prospects for fen meadow restoration on severely degraded fens. *Perspect. Plant Ecol. Evol. Syst.* **2010**, *12*, 245–255. [[CrossRef](#)]
77. Hedberg, P.; Kotowski, W.; Saetre, P.; Mälson, K.; Rydin, H.; Sundberg, S. Vegetation recovery after multiple-site experimental fen restorations. *Biol. Conserv.* **2012**, *147*, 60–67. [[CrossRef](#)]
78. Moosavi, V.; Vafakhah, M.; Shirmohammadi, B.; Behnia, N. A Wavelet-ANFIS Hybrid Model for Groundwater Level Forecasting for Different Prediction Periods. *Water Resour Manag.* **2013**, *27*, 1301–1321. [[CrossRef](#)]
79. Wu, C.; Zhang, X.; Wang, W.; Lu, C.; Zhang, Y.; Qin, W.; Tick, G.R.; Liu, B.; Shu, L. Groundwater level modeling framework by combining the wavelet transform with a long short-term memory data-driven model. *Sci. Total Environ.* **2021**, *783*, 146948. [[CrossRef](#)]
80. Ikram, R.M.A.; Mostafa, R.R.; Chen, Z.; Parmar, K.S.; Kisi, O.; Zounemat-Kermani, M. Water Temperature Prediction Using Improved Deep Learning Methods through Reptile Search Algorithm and Weighted Mean of Vectors Optimizer. *J. Mar. Sci. Eng.* **2023**, *11*, 259. [[CrossRef](#)]
81. Mostafa, R.R.; Kisi, O.; Adnan, R.M.; Sadeghifar, T.; Kuriqi, A. Modeling Potential Evapotranspiration by Improved Machine Learning Methods Using Limited Climatic Data. *Water* **2023**, *15*, 486. [[CrossRef](#)]

**Disclaimer/Publisher’s Note:** The statements, opinions and data contained in all publications are solely those of the individual author(s) and contributor(s) and not of MDPI and/or the editor(s). MDPI and/or the editor(s) disclaim responsibility for any injury to people or property resulting from any ideas, methods, instructions or products referred to in the content.